# $\mathcal{H}_\infty$ State Estimation for PDT-Switched Coupled Neural Networks Under Round-Robin Protocol: A Cooperation-Competition-Based Mechanism

Hao Shen, *Member, IEEE*, Yinsheng Song, Jing Wang, and Ju H. Park, *Senior Member, IEEE*

***Abstract*—This paper is concentrated on the $\mathcal{H}_\infty$ state estimation problem for switched coupled neural networks based on a Takagi-Sugeno fuzzy model. Notably, the time-variant network topology with alternate fast switchings and slow ones is described suitably by a persistent dwell-time rule, and the interactive dynamics with both cooperative properties and antagonistic ones among nodes are featured comprehensively by the switching signed graph. In view of the communication pressures brought by network-induced problems and the requirements in digital control, the round-robin protocol and logarithmic quantization are flexibly integrated for more transmission efficiency and fewer data collisions. Thereafter, by utilizing a relaxed multiple Lyapunov function method and some novel matrix process techniques, sufficient criteria guaranteeing the exponential stability in a globally uniform sense with a prescribed $\mathcal{H}_\infty$ performance level of the estimation error system are established. Finally, the synthesized analysis of the proposed method is presented with an illustrative example.**

***Index Terms*—Switched coupled neural networks, persistent dwell-time, Takagi-Sugeno fuzzy model, cooperation-competition mechanism, round-robin protocol.**

Manuscript received 22 July 2022; revised 26 October 2022; accepted 19 November 2022. Date of publication 24 November 2022; date of current version 23 February 2023. The work of Ju H. Park was supported by the National Research Foundation of Korea (NRF) funded by the Korea government (Ministry of Science and Information and Communications Technology) under Grant 2019R1A5A8080290. This work was supported in part by the National Natural Science Foundation of China under Grants 62173001 and 61873002, in part by the Natural Science Foundation for Excellent Young Scholars of Anhui Province under Grant 2108085Y21, in part by the Major Natural Science Foundation of Higher Education Institutions of Anhui Province under Grant KJ2020ZD28, in part by the Major Technologies Research and Development Special Program of Anhui Province under Grant 202003a05020001, in part by the Key research and development projects of Anhui Province under Grant 202104a05020015, in part by the Open Project of China International Science and Technology Cooperation Base on Intelligent Equipment Manufacturing in Special Service Environment under Grant ISTC2021KF04, in part by the Fundamental Research Funds for the Central Universities under Grant 2021ACOCP05. Recommended for acceptance by Prof. Lin Wang.
*(Corresponding Author: Ju H. Park.)*

Hao Shen is with the AnHui Province Key Laboratory of Special Heavy Load Robot, Anhui University of Technology, Ma'anshan 243032, China, and also with the Key Laboratory of Advanced Control and Optimization for Chemical Processes, Ministry of Education, East China University of Science and Technology, Shanghai 200237, China (e-mail: haoshen10@gmail.com).

Yinsheng Song is with the School of Electrical and Information Engineering, Anhui University of Technology, Ma'anshan 243032, China (e-mail: sys1985525463@163.com).

Jing Wang is with the School of Electrical and Information Engineering, Anhui University of Technology, Ma'anshan 243032, China, and also with the School of Information Science and Engineering, East China University of Science and Technology, Shanghai 200237, China (e-mail: jingwang08@126.com).

Ju H. Park is with the Department of Electrical Engineering, Yeungnam University, Kyongsan 38541, Republic of Korea (e-mail: jessie@ynu.ac.kr).

Digital Object Identifier 10.1109/TNSE.2022.3224390

## I. Introduction

RECENTLY, coupled neural networks (CNNs), as a type of dynamical model that contain lots of intricately interconnected nodes and imitate the structure and function of biological neurons, have exhibited their inherent advantages and potential capability in various fields [1], [2], [3], [4], [5], [6], e.g. pattern recognition [7], smart power grids [8], secure communication [9]. In general, the information interactions among different neurons are regarded as a coordination behavior of CNNs, which can be characterized by a certain network topology (NT). Before further analyzing coupling relationships among nodes, graph theory plays a crucial role in describing the network dynamics [10], [11]. Notice that non-negative graphs are included in the aforesaid achievements, which means that only mutually collaborative interactions among nodes are considered. However, it is universal that there coexist cooperative behaviors and competitive ones in actual networks. Taking the biological networks as an example, the scenario that different individuals must act as both collaborators and antagonists when striving for survival is common, which also signifies that the relationships between neurons of CNNs may be compartmentalized into alliance and adversary. Specifically, the neurons in networks will compete with each other for limited resources inevitably, and these interactions of inhibitory neurons are usually manifested by negative weights in the graph theory. Hence, the research of CNNs with only non-negative graphs has certain constraints in applications. Besides, plenty of achievements have been made in various systems, e.g. switched multi-agents systems [12], heterogeneous multi-agent systems [13], and multiple Euler-Lagrange systems [14] rather than CNNs under the cooperation-competition mechanism, which prompts the investigation demand for CNNs with relevant extensions.

Due to the effect of the external environment or intrinsic factors, the way that the network nodes interact with each other perhaps encounters changes over time or state, which implies that the weighted signed graph may be endowed with switching properties [15]. Such features can be portrayed suitably by switching NT, i.e., some kinds of switching regularities are applied to orchestrate several underlying topologies. In this regard, the research related to switching NT has received much attention. There has been a surge of accomplishments in persistent dwell-time (PDT) switching strategy last decades [16], [17], [18], [19]. In practice, it has been demonstrated that the PDT switching, as a time-dependent switching strategy, is superior in the depiction of the circumstance that fast switchings and slow ones occurs alternatively. For instance, partial electric grids have the characteristics that there is a relatively high load variation frequency in the daytime and a low one at night, and then the power systems may be modeled as the composited systems of multi-mode systems with fast switching and single-mode ones [20]. In addition, nonlinear factors, as an intrinsic property of CNNs, may hinder the establishment of accurate models. With the utilization of a Takagi-Sugeno (T-S) fuzzy model, local linear models are blended by membership functions and a set of IF-THEN rules, which has the capability to approximate the nonlinearity of original systems in the manner of local linearization [21], [22]. At present, fruitful literature have witnessed much effort committed to the robust control and filtering issues for PDT-switched nonlinear systems based on a T-S fuzzy model, see [16], [17], [20]. Unfortunately, relevant issues of the nonlinear CNNs with opposite interactions among nodes and time-variant NT subject to PDT switching have not been explored yet in most existing literature, which perhaps stems from the relatively intractable analysis but arouses us to fill this gap.

Along with the increasing complexity of tasks to be accomplished in the communication networks, the transmission of enormous data and congestion issues for the dynamic networks are stimulating our interest. When the collected data are delivered simultaneously, a great burden caused by hardware and limited network bandwidth resources is bear by network channels, which may result in network-induced problems unavoidably, such as data collisions and disorder, etc. [23], [24], [25], [26] Accordingly, there have been two types of effective solutions in a mass of literature mainly. In detail, one is to reduce the delivery frequency by sampled-data-based control strategies and event-based ones with preset triggering conditions [27], [28], the other is to optimize the occupancy of channels and to allocate the shared network resources reasonably via various scheduling protocols, see [9], [22], [29], [30]. Among different candidates, round-robin protocol (RRP) has been widely employed in global mobile and Ethernet communications to regulate the permission of information acquirement, which also promotes a probe into RRP-based issues. Typically, some RRP-based problems focusing on model-predictive control, robust state estimation, and distributed filtering were tackled in [29], [31], [32] but it should be emphasized PDT-switched nonlinear CNNs are rarely involved in communication-protocol-based literature. In the study of the coupled networks, an important part is to acquire state information since it is indispensable when analyzing the relevant dynamics. Thus, state estimation serves a significant role in crack the nut that the practical node state information is often unavailable or only partially available, and abundant remarkable works have sprung up in past decades, see [18], [33], [34] and the references therein.

Motivated by the above observation, the $\mathcal{H}_\infty$ state estimation issue for nonlinear cooperation-competition CNNs with switching NT in this article is explored. The prominent contributions are as follows:

a) As an attractive attempt, the state estimation issues of the CNNs with nonlinear coefficients are explored based on a T-S fuzzy model, in which a general switching signal with PDT property is adopted to govern the evolution of signed weighted topology. In addition, the complex dynamics involving both cooperative and competitive interactions among individuals are characterized to make the consideration more comprehensive.
b) Considering the network-induced problems and the requirements in digital control, the RRP and logarithmic quantization are embraced for more transmission quality and efficiency and fewer data collisions. In the discrete-time domain, a new fuzzy state estimator is designed to guarantee the exponential stability in global-uniform sense and $\mathcal{H}_\infty$ performance for the PDT-switched nonlinear CNNs under quantization and RRP.
c) For less conservativeness of results, a relaxed multiple Lyapunov function method and some improved matrix processing techniques are utilized to tackle the stability analysis, and a novel candidate function that contains PDT switching and RRP information is established. Furthermore, the validity of presented estimation scheme and the effect of switching signals and quantization on the optimal performance level are explained by an illustrative example.

Notations: The notations throughout this paper are standard except otherwise stated. $\mathcal{R}^a$: the $a$-dimensional Euclidean space; $\mathcal{R}^{a\times b}$: the set of $a \times b$ dimensional matrices; $\|\cdot\|$: Euclidean vector norm; $\mathbb{Z}^+$: the set of non-negative integer; $\mathrm{sgn}(\cdot)$: the sign function; $\mathrm{diag}\{\ldots\}$: the block-diagonal matrix; "$*$" : the term induced by symmetry; $P^T$: the transpose of matrix $P$; $P > 0 (\geq 0)$: positive (semi-positive) definite matrix; $\lambda_{\max}(P)(\lambda_{\min}(P))$: the maximum (minimum) eigenvalue of matrix $P$; $\otimes$: the Kronecker product; $I_n$: the identity matrix; $0_N$: a column vector with all entries being zero.

## II. Problem Formulation

### A. Interaction Graph

Before further discussion, some essential preliminaries on algebraic graph theory [35] ought to be exploited. In this paper, the considered CNN is comprised of $N$ neuron nodes, and their interactions among nodes and switching topology are featured by a weighted signed graph $G_{\delta(k)} \triangleq (\mathcal{M}, \mathcal{T}_{\delta(k)}, \Omega_{\delta(k)})$, where $\delta(k) \in \mathcal{S} \triangleq \{1, 2, \ldots, S\}$ denotes a switching signal, and $\mathcal{M} \triangleq \{1, 2, \ldots, N\}$, $\mathcal{T}_{\delta(k)} \subseteq \mathcal{M} \times \mathcal{M}$, and $\Omega_{\delta(k)} \triangleq [h_{ij}^{\delta(k)}]_{N\times N}$

represent the node set, the edge set and the weighted adjacency matrix, respectively. As is mentioned that the existing interactions among nodes, not only the collaborative but the antagonistic ones, should be taken into account, which can be achieved by edges with the positive or negative weights. In addition, the entry $h_{ij}^{\delta(k)}$ symbolizes the connection weights between node $i$ and $j$, and $(j,i) \in \mathcal{T}_{\delta(k)} \Leftrightarrow h_{ij}^{\delta(k)} \neq 0$; Otherwise, $h_{ij}^{\delta(k)} = 0$. Specifically, the self-edges $(i,i)$ are not available, that is $h_{ii}^{\delta(k)} = 0$ for $i \in \mathcal{M}$, $\delta(k) \in \mathcal{S}$. Hence, for the topology subject to $\delta(k)$, the Laplacian matrix $\mathcal{L}_{\delta(k)} \triangleq [l_{ij}^{\delta(k)}]_{N\times N}$ of graph $G_{\delta(k)}$ can be provided as $\mathcal{L}_{\delta(k)}=\mathcal{J}_{\delta(k)}-\Omega_{\delta(k)}$, where $\mathcal{J}_{\delta(k)} \triangleq \mathrm{diag}\{d_{\delta(k)}^{(1)},\ldots,d_{\delta(k)}^{(N)}\}$ and $d_{\delta(k)}^{(i)} \triangleq \sum_{j=1}^{N} |h_{ij}^{\delta(k)}|$.

*Definition 1 ( [36]):* For $\delta(k) \in \mathcal{S}$, a weighted signed graph $G_{\delta(k)}$ serves as the structurally balanced one provided that the node set $\mathcal{M}$ consists of two disjoint subsets $\mathcal{M}_1$ and $\mathcal{M}_2(\mathcal{M}_1 \cup \mathcal{M}_2 = \mathcal{M}, \mathcal{M}_1 \cap \mathcal{M}_2 = \emptyset)$, such that $h_{ij}^{\delta(k)} \geq 0$ for $\forall i,j \in \mathcal{M}_\varpi(\varpi \in \{1,2\})$ and $h_{ij}^{\delta(k)} \leq 0$ for $\forall i \in \mathcal{M}_\pi$, $\forall j \in \mathcal{M}_\varpi, i \neq j$ $(\pi,\varpi \in \{1,2\})$.

*Lemma 1 ( [37]):* Based on Definition 1, if the weighted signed graph $G_{\delta(k)}$ is structurally balanced, then there exists a diagonal matrix $\Phi \triangleq \mathrm{diag}\{\varphi_1,\ldots,\varphi_N\}$ with $\varphi_i \in \{1,-1\}$, $i \in \mathcal{M}$, which is applied for the gauge transformation and satisfies $\overrightarrow{\Omega}_{\delta(k)} \triangleq \Phi\Omega_{\delta(k)}\Phi$ with $\overrightarrow{\Omega}_{\delta(k)} \triangleq [|h_{ij}^{\delta(k)}|]_{N\times N}$.

*Remark 1:* Note that the Laplacian matrix $\mathcal{L}_{\delta(k)}$ is not a zero-row-sum matrix, which brings more difficulty for the subsequent analysis than traditional unsigned graph. The matrix $\Phi$ mentioned in Lemma 1 is in a position to transform $\mathcal{L}_{\delta(k)}$ into the zero-row-sum matrix $\overline{\mathcal{L}}_{\delta(k)} = \Phi\mathcal{L}_{\delta(k)}\Phi = [\bar{l}_{ij}^{\delta(k)}]_{N\times N}$ for $\forall\delta(k) \in \mathcal{S}$.

## B. Node Dynamic With Switching Topology

Considering the antagonistic interactions, switching NT, and nonlinear coefficients in CNNs, the dynamics of node $i$ can be expressed based on the following T-S fuzzy model as:

*Plant rule* $\alpha$: IF $\theta_1(k)$ is $\mathcal{X}_{\alpha 1}$, $\theta_2(k)$ is $\mathcal{X}_{\alpha 2},\ldots,\theta_b(k)$ is $\mathcal{X}_{\alpha b}$, THEN

$$\begin{cases} x_i(k+1) = A_\alpha x_i(k) + B_\alpha f(x_i(k)) + E_{i,\alpha}\omega(k) \\ \qquad\qquad + c\sum_{j=1}^{N}\left|h_{ij}^{\delta(k)}\right|\left(\mathrm{sgn}\left(h_{ij}^{\delta(k)}\right)x_j(k) - x_i(k)\right) \\ y_i(k) = \varphi_i D x_i(k) \\ z_i(k) = \varphi_i F_\alpha x_i(k), i=1,\ldots,N \end{cases} \tag{1}$$

where $\alpha = 1,\ldots,r$, and $r$ is the number of fuzzy rules; $\theta_1(k)$, $\theta_2(k),\ldots,\theta_\beta(k)$ $(\beta = 1,\ldots,b)$ denote the premise variables; $\mathcal{X}_{\alpha\beta}$ represents the fuzzy sets; $\delta(k) \in \mathcal{S}$ is the constant function satisfying the PDT switching property, which is right-continuous and piecewise; $x_i(k) \in \mathcal{R}^{n_x}$, $y_i(k) \in \mathcal{R}^{n_y}$, and $z_i(k) \in \mathcal{R}^{n_z}$ refer to the state vectors, measurement output and output vectors of node $i$, respectively. $c > 0$ is the coupling strength; $\omega(k)$ expresses the external disturbance input belonging to $l_2[0,\infty)$; $f(x_i(k))$ indicates the activation function of neuron; $A_\alpha \triangleq \mathrm{diag}\{a_{1\alpha},a_{2\alpha},\ldots,a_{\hbar\alpha}\} \in \mathcal{R}^{n_x\times n_x}$, in which $a_{\ell\alpha} > 0$ stands for the charging time of neuron $\ell$, $\ell \in \mathbb{N} \triangleq \{1,2,\ldots,\hbar\}$, $\hbar$ is the number of neurons; $B_\alpha \in \mathcal{R}^{n_x\times n_x}$ signifies the weight matrix of connection; $E_{i,\alpha} \in \mathcal{R}^{n_x\times n_w}$, $D \in \mathcal{R}^{n_y\times n_x}$, $F_\alpha \in \mathcal{R}^{n_z\times n_x}$. All the coefficient matrices are known ones with appropriate dimensions.

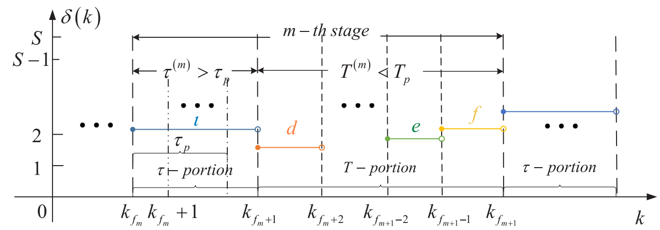


Fig. 1. Possible scenario of PDT switching $\delta(k)$ in the $m$-th stage.

Through the approach of weighted defuzzification, the overall system can be restated as

$$\begin{cases} x_i(k+1) = \sum_{\alpha=1}^{r}\xi_\alpha(\theta(k))(A_\alpha x_i(k) \\ \qquad\qquad + B_\alpha f(x_i(k)) + E_{i,\alpha}\omega(k)) \\ \qquad\qquad + c\sum_{j=1}^{N}\left|h_{ij}^{\delta(k)}\right|\left(\mathrm{sgn}\left(h_{ij}^{\delta(k)}\right)x_j(k) - x_i(k)\right) \\ y_i(k) = \varphi_i D x_i(k) \\ \quad z_i(k) = \sum_{\alpha=1}^{r}\xi_\alpha(\theta(k))(F_\alpha\varphi_i x_i(k)), i=1,\ldots,N \end{cases} \tag{2}$$

where $\xi_\alpha(\theta(k))$ is the standard form of membership function defined as

$$\xi_\alpha(\theta(k)) = \frac{\Pi_{\beta=1}^{b}\mathcal{X}_{\alpha\beta}(\theta_\beta(k))}{\sum_{\alpha=1}^{r}\Pi_{\beta=1}^{b}\mathcal{X}_{\alpha\beta}(\theta_\beta(k))}$$

in which $\mathcal{X}_{\alpha\beta}(\theta_\beta(k))$ describes the grade of membership of $\theta_\beta(k)$ in $\mathcal{X}_{\alpha\beta}$. Denote $\overline{\xi}_\alpha \triangleq \xi_\alpha(\theta(k))$, $\sum_{\alpha=1}^{r}\overline{\xi}_\alpha = 1$, and $\overline{\xi}_\alpha \geq 0$ always hold for all $k$.

After that, the relevant complement of the PDT switching should be mentioned.

*Definition 2 ( [18]):* For two scalars $T_P > 0$ and $\tau_p > 0$, the signal $\delta(k)$ embodying the following switching characteristics is said to comply with the PDT switching strategy: (i) The value of $\delta(k)$ is a constant on each one of innumerable non-adjacent intervals of length no less than a PDT $\tau_p$. (ii) The interval named as $T$-portion of length no larger than a period of persistence $T_p$ separates the intervals defined above, on which the value of $\delta(k)$ is variable.

As the sketch pertaining to $m$-th stage shown in Fig. 1. $k_{f_m}$, $k_{f_m+1},\ldots,$ $k_{f_{m+1}-1}$, $k_{f_{m+1}}$ are the switching instants, and $k_{f_m}+1$ denotes the next sampling instant after $k_{f_m}$. Overall, The entire $m$-th stage consists of $\tau$-portion and $T$-portion, which are called fast switching and slow one, and their duration is $\tau^{(m)} \geq \tau_p$ and $T^{(m)} = T_d + T_e + \ldots + T_f \leq T_p$, respectively, in which $T_x$ $(x = d,e,\ldots,f)$ implies the running time of each activated element in the $T$-portion, respectively. As stated in [18], with the employment of PDT switching in the interval $[t,k)$, the switching times $\mathscr{A}(t,k)$ satisfies

$$\mathscr{A}(t,k) \leq \left(\frac{k-t}{T_p+\tau_p}+1\right)(T_p+1). \tag{3}$$

*Remark 2:* It should be stressed that the dwell-time (DT) switching and the average DT (ADT) one, as two other time-dependent strategies except the PDT switching, have appeared in the earlier references. The former requires the running time of each subsystem to be no less than $\tau_d > 0$, which causes its lack of fast switching, and the latter has the switching times $\mathscr{A}(t,k) \le \frac{k-t}{\tau_a} + N_0$, where $\tau_a > 0$ and $N_0 > 0$, while such $N_0$ to limit fast switching frequency disappears in the PDT switching. Specially, denoting the sets of switching signals with DT, ADT, PDT property as $\mathcal{S}_{\mathcal{D}}(\tau_d)$, $\mathcal{S}_{\mathcal{A}}(\tau_a, N_0)$, $\mathcal{S}_{\mathcal{P}}(\tau_p, T_p)$, respectively. $\mathcal{S}_{\mathcal{D}}(\tau_d) = \mathcal{S}_{\mathcal{A}}(\tau_a, 1) = \mathcal{S}_{\mathcal{P}}(\tau_p, 0) \subset \mathcal{S}_{\mathcal{A}}(\tau_a, N_0) \subset \mathcal{S}_{\mathcal{P}}(\overline{h}\tau_p, T_p)$ can be deduced provided that $\tau_d = \tau_a = \tau_p$, where $N_0 \ge 1$, $0 < \overline{h} < 1$ and $T_p \triangleq \overline{h}\tau_p(\frac{N_0-1}{1-\overline{h}})$, which means that the PDT switching is more flexible and general than the two other strategies.

Next, some appropriate assumptions are made with respect to the signed graph $G_{\delta(k)}$ and activation function $f(\cdot)$.

*Assumption 1:* The signed graph $G_{\delta(k)}$ belonging to neural network (1) has the structural balance for $\forall \delta(k) \in \mathcal{S}$.

*Assumption 2:* For $i \in \mathbb{N}$, $f_i(\cdot)$ is a bounded and continuous odd activation function, which satisfies

$$\nu_i^- \le \frac{f_i(\varepsilon_1) - f_i(\varepsilon_2)}{\varepsilon_1 - \varepsilon_2} \le \nu_i^+, \varepsilon_1, \varepsilon_2 \in \mathcal{R}^{n_x}, (\varepsilon_1 \ne \varepsilon_2) \tag{4}$$

where $f_i(0) = 0$. $\nu_i^-$ and $\nu_i^+$ are known real scalars.

Based on Lemma 1, $\Phi$ is introduced for the purpose of vector transformation, and it is not difficult to find that matrix $\overline{\mathcal{L}}_m \triangleq \Phi \mathcal{L}_m \Phi$ is zero-row-sum for $\forall m \triangleq \delta(k) \in \mathcal{S}$. Define $\overline{x}_i \triangleq \varphi_i x_i$, the dynamic of node $i$ for the CNN (2) is depicted as

$$\begin{cases} \overline{x}_i(k+1) = \sum_{\alpha=1}^r \overline{\xi}_\alpha (A_\alpha \overline{x}_i(k) + B_\alpha f(\overline{x}_i(k)) \\ \qquad\qquad + \varphi_i E_{i,\alpha} \omega(k)) - c\sum_{j=1}^N \overline{l}_{ij}^m \overline{x}_j(k) \\ y_i(k) = D\overline{x}_i(k) \\ z_i(k) = \sum_{\alpha=1}^r \overline{\xi}_\alpha (F_\alpha \overline{x}_i(k)), i = 1, \ldots, N. \end{cases} \tag{5}$$

*Remark 3:* It is essential to embrace the accuracy and complexity issues when linearizing the target systems. In this paper, the switched CNNs with nonlinear coefficients are explored based on a T-S fuzzy model, by which the obvious advantages are its matured applications. The other methods have also stimulated our intense interests, e.g. a novel approximation approach in [38]. However, more potential complexity may be brought rather than the T-S fuzzy model. For less complexity and to highlight the competition-cooperation and switching features of CNNs, our attention mainly centered on a classic T-S fuzzy method. Undeniably, the extension with other fuzzy methods is still worthy of further exploration.

### C. Quantized Data Under the RRP

To protect communication environments from network-induced phenomena as possible, a logarithmic quantizer and RRP are adopted to process the measured data in this paper.

Assume that the sensors existing in the investigated plant are divided into $N$ nodes, then $y(k) \triangleq [y_1^T(k) \ldots y_N^T(k)]^T$, in which $y_n(k)$ is the measurement output corresponding to the $n$th sensor node ($n \in \{1, 2, \ldots, N\}$). A logarithmic quantizer is denote as $Q_n(y_n(k)) \triangleq [q_n(y_n^1(k)) \ldots q_n(y_n^{n_y}(k))]^T$, in which $y_n^p(k)$ is the $p$th element of $y_n(k)$ ($p \in \{1, 2, \ldots, n_y\}$). For each $q_n(y_n^p(k))$, the prospective quantized level can be realized as

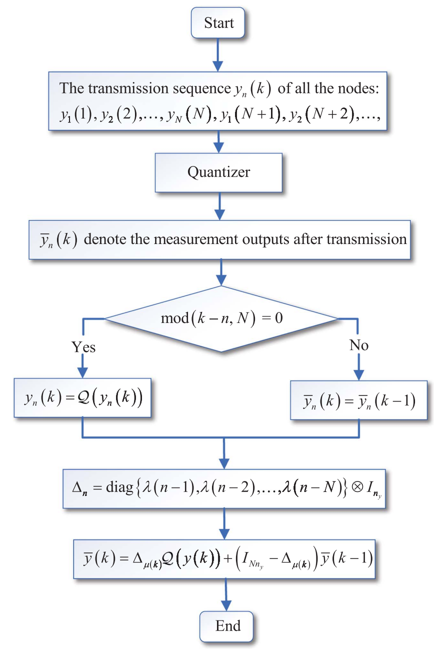


Fig. 2. Signal transmission of the quantized measurement outputs under the RRP.

$$L_n \triangleq \left\{ \pm l_n^{(t)} \mid l_n^{(t)} = (\eta_n)^t l_n^{(0)}, t = 0, \pm 1, \pm 2, \ldots \right\} \cup \{0\}$$

where $l_n^{(0)}$ denotes the initial value of quantizer point $l_n^{(t)}$ and $\eta_n \in (0, 1)$ is the quantization density on which the quantizer performs, and $\eta \triangleq \mathrm{diag}\{\eta_1, \ldots, \eta_N\}$, then we have

$$q_n(y_n^p(k)) \triangleq \begin{cases} l_n^{(t)}, & \frac{l_n^{(t)}}{1+\overline{\kappa}_n} \le y_n^p(k) \le \frac{l_n^{(t)}}{1-\overline{\kappa}_n} \\ 0, & y_n^p(k) = 0 \\ -q_n(-y_n^p(k)), & y_n^p(k) < 0 \end{cases}$$

with $\overline{\kappa}_n \triangleq \frac{1-\eta_n}{1+\eta_n}$. For each node, its quantization error can be portrayed as

$$\mathcal{Q}_n(y_n(k)) - y_n(k) = \upsilon_n(k) y_n(k) \tag{6}$$

where $\upsilon_n(k)$ is the actual error belonging to the $n$th sensor node, and then the overall quantization error is generalized as

$$\mathcal{Q}(y(k)) - y(k) = \triangle(k) y(k) \tag{7}$$

with $\triangle(k) \triangleq \mathrm{diag}\{\upsilon_1(k), \ldots, \upsilon_N(k)\} \otimes I_{n_y}$, and it satisfies that $\triangle(k) \le \Gamma \triangleq \mathrm{diag}\{\overline{\kappa}_1, \ldots, \overline{\kappa}_N\} \otimes I_{n_y} \le I_{Nn_y}$.

For convenience, define the Kronecker delta function $\lambda(\cdot)$ satisfying: (1) $\lambda(n) = 1$ when $n = 0$; (2) $\lambda(n) = 0$ when $n \ne 0$. Furthermore, in order to exhibit the characteristic of the such protocol, the following principle, $\mu(k) \triangleq \mathrm{mod}(k - 1, N) + 1$ with $\mu(k) \in \mathbb{N}$, is established for determining the selected sensor node $\mu(k)$ at time $k$. Then, as described in Fig. 2, for the aforesaid $y(k)$, assume that the information of its $n$th node $y_n(k)$ is allocated to update as $\overline{y}_n(k)$ at time $k$, and then the overall transferred data accepted by the state estimator can be obtained as $\overline{y}(k) = [\overline{y}_1^T(k) \ldots \overline{y}_N^T(k)]^T$, in which the allowable value of $\overline{y}_n(k)$ is judged by the decision-making mechanism.

*Remark 4:* The data collision and disorder caused by massive information flowing in data links can be alleviated, which benefits from the simple and effective RRP such that the transmission sequence of sensor nodes is arranged reasonably. Specifically, the transfer permission of each node is granted, and all nodes are traversed in a fixed order periodically and only one gets access to updating its data at a time.

*Remark 5:* The raw data obtained from plants should be quantized before sending to the next segment because of limited channels and ubiquitous existence of digital signal processing equipment. Wherein, the density $\eta_n$ is a critical index in the quantization, and the smaller value of $\eta_n$ owns, the more efficiency but less accuracy there are. The effect of $\eta_n$ on the $\mathcal{H}_\infty$ performance level will be further analyzed in the subsequent section.

### D. State Estimator Design

Considering the above-mentioned analysis for the dynamic of node $i$ and denoting $\widetilde{x}(k) \triangleq [\,\overline{x}^T(k) \quad \overline{y}^T(k-1)]^T$, the networks consisting of $N$ coupled node with the RRP are given as

$$\begin{cases} \widetilde{x}(k+1) = \sum_{\alpha=1}^{r} \overline{\xi}_\alpha \Big(\overline{A}^\alpha_{m,\mu(k)} \widetilde{x}(k) + \overline{B}_\alpha f(\widetilde{x}(k)) \\ \qquad\qquad +\overline{E}_\alpha \omega(k)\Big) \\ \overline{y}(k) = \overline{D}_{\mu(k)} \widetilde{x}(k) \\ z(k) = \sum_{\alpha=1}^{r} \overline{\xi}_\alpha \big[\overline{F}_\alpha \widetilde{x}(k)\big] \end{cases} \tag{8}$$

where

$$\begin{aligned} \overline{A}^\alpha_{m,\mu(k)} &\triangleq \begin{bmatrix} A^\alpha_m & 0 \\ \phi_{\mu(k)} & I_{Nn_y} - \triangle_{\mu(k)} \end{bmatrix} \\ \overline{B}_\alpha &\triangleq \begin{bmatrix} I_N \otimes B_\alpha & 0 \\ 0 & 0 \end{bmatrix}, \overline{E}_\alpha \triangleq \begin{bmatrix} \Phi \otimes I_N E_\alpha \\ 0 \end{bmatrix} \\ A^\alpha_m &\triangleq I_N \otimes A_\alpha - c\overline{\mathcal{L}}_m \otimes I_{n_x} \\ E_\alpha &\triangleq \Big[E^T_{1,\alpha} \ldots E^T_{N,\alpha}\Big]^T, \overline{F}_\alpha \triangleq [\, I_N \otimes F_\alpha \quad 0\,] \\ \overline{D}_{\mu(k)} &\triangleq \big[\, \phi_{\mu(k)} \quad I_{Nn_y} - \triangle_{\mu(k)} \,\big] \\ \phi_{\mu(k)} &\triangleq \triangle_{\mu(k)} \,\big(I_{Nn_y} + \triangle(k)\big)(I_N \otimes D). \end{aligned}$$

With the aim of obtaining the state information of networks (8), the following fuzzy state estimator is constructed

*Estimator rule* $\alpha$: IF $\theta_1(k)$ is $\mathcal{X}_{\alpha 1}$, $\theta_2(k)$ is $\mathcal{X}_{\alpha 2}$, ..., $\theta_b(k)$ is $\mathcal{X}_{\alpha \mathrm{b}}$, THEN

$$\begin{cases} \widehat{x}(k+1) = \sum_{\alpha=1}^{r} \overline{\xi}_\alpha \Big(\overline{A}^\alpha_{m,\mu(k)} \widehat{x}(k) + \overline{B}_\alpha f(\widehat{x}(k)) \\ \qquad\qquad + \sum_{\beta=1}^{r} \overline{\xi}_\beta K^\beta_m \big(\overline{y}(k) - \overline{D}_{\mu(k)} \widehat{x}(k)\big)\Big) \\ \widehat{z}(k) = \sum_{\alpha=1}^{r} \overline{\xi}_\beta \big(\overline{F}_\alpha \widehat{x}(k)\big) \end{cases} \tag{9}$$

where $\widehat{x}(k) \triangleq [\,\widehat{x}_1^T(k) \quad \widehat{x}_2^T(k)\,]^T$ with $\widehat{x}_1(k) \in \mathcal{R}^{n_x N}$, $\widehat{x}_2(k) \in \mathcal{R}^{n_y N}$ being the estimation of $\overline{x}(k)$ and $\overline{y}(k-1)$, respectively. $\widehat{z}(k) \in \mathcal{R}^{n_z N}$ is the output of estimator. For $\forall m \triangleq \delta(k) \in \mathcal{S}$, $K^\beta_m \in \mathcal{R}^{(n_x+n_y)N \times n_x N}$ denotes the estimator gains to be determined.

Define the estimator error $e(k) \triangleq \widetilde{x}(k) - \widehat{x}(k)$, $\widetilde{z}(k) \triangleq z(k) -\widehat{z}(k)$, $\overline{f}(e(k)) \triangleq f(\widetilde{x}(k)) - f(\widehat{x}(k))$, then the estimation error system (EES) can be written as follows

$$\begin{cases} e(k+1) = \sum_{\alpha=1}^{r} \sum_{\beta=1}^{r} \overline{\xi}_\alpha \overline{\xi}_\beta \Big(\Big(\overline{A}^\alpha_{m,\mu(k)} - K^\beta_m \overline{D}_{\mu(k)}\Big) e(k) \\ \qquad +\overline{B}_\alpha \overline{f}(e(k)) + \overline{E}_\alpha \omega(k)\Big) \\ \widetilde{z}(k) = \sum_{\alpha=1}^{r} \sum_{\beta=1}^{r} \overline{\xi}_\alpha \overline{\xi}_\beta \big(\overline{F}_\alpha e(k)\big) \end{cases} \tag{10}$$

which has a compact form as

$$\begin{cases} e(k+1) = \mathbb{A}^{\alpha\beta}_{m,\mu(k)} e(k) + \mathbb{B}^\alpha \overline{f}(e(k)) + \mathbb{E}^\alpha \omega(k) \\ \widetilde{z}(k) = \mathbb{F}^\alpha e(k) \end{cases} \tag{11}$$

where

$$\mathbb{A}^{\alpha\beta}_{m,\mu(k)} \triangleq \sum_{\alpha=1}^{r} \sum_{\beta=1}^{r} \overline{\xi}_\alpha \overline{\xi}_\beta \Big(\overline{A}^\alpha_{m,\mu(k)} - K^\beta_m \overline{D}_{\mu(k)}\Big)$$

$$\mathbb{B}^\alpha \triangleq \sum_{\alpha=1}^{r} \overline{\xi}_\alpha \overline{B}_\alpha, \mathbb{E}^\alpha \triangleq \sum_{\alpha=1}^{r} \overline{\xi}_\alpha \overline{E}_\alpha, \mathbb{F}^\alpha \triangleq \sum_{\alpha=1}^{r} \overline{\xi}_\alpha \overline{F}_\alpha.$$

The stability and performance of the EES (11) refer to some necessary definitions and lemmas that are defined as follows.

*Definition 3 ( [16]):* With the condition $\omega(k) \equiv 0$, the resulting EES (11) is globally uniformly exponentially stable (GUES) if there exist scalars $\widehat{\alpha} \in (0, \infty)$ and $\overline{\sigma} \in (0, 1)$, such that the inequality $\|e(k)\|^2 \leq \widehat{\alpha}\overline{\sigma}^{k-k_0} \|e(k_0)\|^2$, $\forall k \geq k_0$ holds for all initial conditions.

*Definition 4 ( [16]):* The EES (11) is GUES with an $\mathcal{H}_\infty$ performance level $\overline{\gamma}$ if the following conditions are satisfied: (i) The system (11) is GUES; (ii) For $\forall \omega(k) \in l_2[0, \infty)$, there exist a scalar $\overline{\gamma} \in (0, \infty)$ such that the inequality $\sum_{q=0}^{\infty} \|\widetilde{z}(q)\|^2 \leq \overline{\gamma}^2 \sum_{q=0}^{\infty} \|\omega(q)\|^2$ holds under zero-initial conditions.

*Lemma 2 ( [22]):* For matrix $\Upsilon_{\alpha\beta}$, $\alpha$, $\beta = 1, 2, \ldots, r$, the following inequality $\sum_{\alpha=1}^{r} \sum_{\beta=1}^{r} \overline{\xi}_\alpha \overline{\xi}_\beta \Upsilon_{\alpha\beta} < 0$ holds, if $\Upsilon_{\alpha\alpha} < 0$ and $\frac{1}{r-1} \Upsilon_{\alpha\alpha} + \frac{1}{2}(\Upsilon_{\alpha\beta} + \Upsilon_{\beta\alpha}) < 0, (\alpha \neq \beta)$.

*Lemma 3 ( [16]):* Given real matrices $\mathcal{H}$, $\mathcal{I}$ and $\mathcal{F}$ with proper dimensions, in which $\mathcal{F}^T\mathcal{F} \leq \mathcal{I}$, for any scalar $\zeta > 0$ there always holds $\mathcal{H}^T\mathcal{F}\mathcal{I} + \mathcal{I}^T\mathcal{F}^T\mathcal{H} \leq \zeta^{-1}\mathcal{H}^T\mathcal{H} + \zeta\mathcal{I}^T\mathcal{I}$.

## III. Main Results

In this section, more attention is paid to analyzing the feasibility of the proposed estimation scheme for the studied fuzzy switched CNNs. Several criteria guaranteeing the globally uniform exponential stability with the $\mathcal{H}_\infty$ property of the EES (11) are provided first. Presently, the concrete forms of aim estimator gains are displayed in the following Theorem 2. For simplicity, we denote

$$\begin{aligned}&\varXi_k \triangleq \tilde{z}^T(k)\tilde{z}(k) - \gamma^2\omega^T(k)\omega(k)\\&\psi_1 \triangleq \min_{m\in\mathcal{S}}\left\{\lambda_{\min}\left(\mathcal{P}_{m,\mu(k)}\right)\right\},\ \psi_2 \triangleq \max_{\mathrm{m}\in\mathcal{S}}\left\{\lambda_{\max}\left(\mathcal{P}_{\mathrm{m},\mu(\mathrm{k})}\right)\right\}\\&\overline{\varsigma} \triangleq \max_{k\geq k_0, m\in\mathcal{S}}\left\{\varsigma^{\frac{m}{k-k_0+1}}\right\},\ \varsigma \triangleq \max_{m\in\mathcal{S}}\left\{\rho^{T^{(m)}+1}\sigma^{T^{(m)}+\tau_p}\right\}\\&k_0 \triangleq k_{f_1},\ \overline{\rho} \triangleq \rho^{\left(\frac{1}{T_p+\tau_p}+1\right)\left(T_p+1\right)},\ \overline{\sigma} \triangleq \sigma\rho^{\frac{T_p+1}{T_p+\tau_p}}.\end{aligned}$$

*Theorem 1:* A candidate Lyapunov function form is considered as below

$$V_{\delta(k)}(e(k), \mu(k)) \triangleq e^T(k)\mathcal{P}_{\delta(k),\mu(k)}e(k). \tag{12}$$

Given scalars $\gamma > 0$, $\rho > 1$ and $0 < \sigma < 1$, $T_p > 0$, $\tau_p > 0$, if there exist symmetric matrices $\mathcal{P}_{m,\mu(k)} > 0$ for $\forall m \in \mathcal{S}$, $\forall t \in \mathbb{Z}^+$, and the following inequalities hold

$$V_{\delta(k)}(e(k+1), \mu(k+1)) \leq \sigma V_{\delta(k)}(e(k), \mu(k)) + \varXi_k \tag{13}$$

$$\begin{aligned}&V_{\delta\left(k_{f_m+t}\right)}\left(e\left(k_{f_m+t}\right), \mu\left(k_{f_m+t}\right)\right)\\&\leq \rho V_{\delta\left(k_{f_m+t}\right)}\left(e\left(k_{f_m+t}\right), \mu\left(k_{f_m+t-1}\right)\right)\end{aligned} \tag{14}$$

$$\sigma^{\left(T_p+\tau_p\right)}\rho^{\left(T_p+1\right)} < 1 \tag{15}$$

then the EES (11) is GUES with an expected $\mathcal{H}_\infty$ performance level $\overline{\gamma} \triangleq \gamma\sqrt{\overline{\rho}\frac{1-\sigma}{1-\overline{\sigma}}}$.

*Proof:* With consideration of $k \in [k_{f_m}, k_{f_{m+1}})$, combining with (13) and (14), under $\omega(k) \equiv 0$, the following inequality can be deduced that

$$\begin{aligned}&V_{\delta\left(k_{f_{m+1}}\right)}\left(e\left(k_{f_{m+1}}\right), \mu\left(k_{f_{m+1}}\right)\right)\\&\leq \rho\sigma\left(V_{\delta\left(k_{f_{m+1}-1}\right)}\left(e\left(k_{f_{m+1}}-1\right), \mu\left(k_{f_{m+1}}-1\right)\right)\right)\\&\leq \rho^{\mathscr{A}\left(\mathfrak{k}_{\mathrm{f_{m+1}}}, \mathfrak{k}_{\mathrm{f_m}}\right)}\sigma^{k_{f_{m+1}}-k_{f_m}}\left(V_{\delta\left(k_{f_m}\right)}\left(e\left(k_{f_m}\right), \mu\left(k_{f_m}\right)\right)\right)\\&\leq \varsigma\left(V_{\delta\left(k_{f_m}\right)}\left(e\left(k_{f_m}\right), \mu\left(k_{f_m}\right)\right)\right).\end{aligned}$$

For any $\rho \in (1, \infty)$ and $\sigma \in (0, 1)$, it can be concluded that $\varsigma \in (0, 1)$ holds. Afterwords, we have

$$\begin{aligned}&V_{\delta(k)}(e(k), \mu(k))\\&\leq \rho^{\mathscr{A}\left(\mathfrak{k}_{\mathrm{f_m}}, \mathfrak{k}\right)}\sigma^{k-k_{f_m}}\varsigma^{m-1}\left(V_{\delta\left(k_{f_1}\right)}\left(e\left(k_{f_1}\right), \mu\left(k_{f_1}\right)\right)\right)\\&\leq \rho^{T_p+1}\varsigma^{m-1}\left(V_{\delta\left(k_{f_1}\right)}\left(e\left(k_{f_1}\right), \mu\left(k_{f_1}\right)\right)\right)\\&\leq \rho^{T_p+1}\overline{\varsigma}^{k-k_0+1}\varsigma^{-1}\left(V_{\delta\left(k_{f_1}\right)}\left(e\left(k_{f_1}\right), \mu\left(k_{f_1}\right)\right)\right).\end{aligned} \tag{16}$$

Consider (12), then one has

$$\psi_1\|e(k)\|^2 \leq V_{\delta(k)}(e(k), \mu(k)) \leq \psi_2\|e(k_0)\|^2,$$

meanwhile, combining with (16), it can be got that

$$\|e(k)\|^2 \leq \widehat{\alpha}\overline{\sigma}^{k-k_0}\|e(k_0)\|^2$$

with $\widehat{\alpha} \triangleq \frac{\psi_2\overline{\varsigma}}{\psi_1\varsigma}\rho^{T_p+1}$, which proves that the EES (11) is GUES.

On the other, with $V_{\delta(k)}(e(k), \mu(k)) \geq 0$ and the zero-initial conditions, it can be inferred from (13) and (14) that

$$\sum_{q=k_0}^{k-1}\rho^{\mathscr{A}(q,k)}\sigma^{k-q+1}\varXi_q \geq 0$$

which implies

$$\sum_{k=k_0+1}^{\infty}\sum_{q=k_0}^{k-1}\rho^{\mathscr{A}(q,k)}\sigma^{k-q+1}\varXi_q \geq 0. \tag{17}$$

With the equal ratio summation formula being drawn on, one can further obtain from (17) that

$$\sum_{q=0}^{\infty}\|\tilde{z}(q)\|^2 \leq \overline{\gamma}^2\sum_{q=0}^{\infty}\|\omega(q)\|^2$$

which means that the prescribed $\mathcal{H}_\infty$ performance is satisfied. It completes the proof. ■

*Remark 6:* To obtain less conservative results, two scalars $\rho$ and $\sigma$ are taken into consideration in this paper. $\rho > 1$ is the decay rate corresponding to the switching instant, which can ensure the energy function value of the next activated element can be higher than the value of the previous one in this instant. Meanwhile, $0 < \sigma < 1$ is the attenuation rate when the samplings occur, which guarantees the energy function decreases strictly during the running time. Although the energy function does not decrease monotonically in the entire $m$-th stage, the goal of stability is achieved. More results about the effect of $\rho$ and $\sigma$ on the $\mathcal{H}_\infty$ performance will be given in the illustration example section.

*Theorem 2:* Given scalars $\gamma > 0$, $0 < \sigma < 1$, $\rho > 1$, diagonal matrices $N_m$, if there exist symmetric matrices $\mathcal{P}_{m,\mu(k)} > 0$, diagonal matrices $\Lambda_m > 0$ and $R_{1m} \in \mathcal{R}^{n_xN\times n_xN}$, $R_{2m} \in \mathcal{R}^{n_yN\times n_yN}$, $\overline{K}^{\beta}_{1m} \in \mathcal{R}^{n_xN\times n_yN}$, $\overline{K}^{\beta}_{2m} \in \mathcal{R}^{n_yN\times n_yN}$ and a positive scalar $\zeta$, the following inequalities and condition (15) hold for $\forall m, \epsilon_1, \epsilon_2 \in \mathcal{S}$ and $\forall\alpha, \beta \in \{1, 2, \ldots, r\}$

$$\mathcal{P}_{\epsilon_1,\mu(k)} \leq \rho\mathcal{P}_{\epsilon_2,\mu(k)}(\epsilon_1 \neq \epsilon_2) \tag{18}$$

$$\Upsilon^{\alpha\alpha}_{m,\mu(k)} < 0 \tag{19}$$

$$\frac{2}{r-1}\Upsilon^{\alpha\alpha}_{m,\mu(k)} + \Upsilon^{\alpha\beta}_{m,\mu(k)} + \Upsilon^{\beta\alpha}_{m,\mu(k)} < 0 \tag{20}$$

where

$$\Upsilon^{\alpha\beta}_{m,\mu(k)} \triangleq \begin{bmatrix} \Theta^{\alpha}_{1\,m,\mu(k)} & \Theta^{\alpha\beta}_{2\,m,\mu(k)} \\ * & \Theta^{\beta}_{3\,m,\mu(k)} \end{bmatrix}$$

$$\Theta^{\alpha}_{1\,m,\mu(k)} \triangleq \begin{bmatrix} \Phi^{\alpha}_{1m,\mu(k)} & 0 \\ * & -\gamma^2 I \end{bmatrix}$$

$$\Theta^{\beta}_{3\,m,\mu(k)} \triangleq \begin{bmatrix} \overline{\mathcal{P}}_{m,\mu(k+1)} & Y^{\beta}_{m} \\ * & -\zeta^{-1} I \end{bmatrix}$$

$$\Theta^{\alpha\beta}_{2\,m,\mu(k)} \triangleq \begin{bmatrix} \Phi^{\alpha\beta}_{2m,\mu(k)} & 0 \\ \Phi^{\alpha}_{3m} & 0 \end{bmatrix}, \overline{K}^{\beta}_{m} \triangleq \begin{bmatrix} \overline{K}^{\beta}_{1m} \\ \overline{K}^{\beta}_{2m} \end{bmatrix}$$

$$\Phi^{\alpha\beta}_{2\,m,\mu(k)} \triangleq \left(\mathcal{R}_m \mathcal{A}^{\alpha}_{m,\mu(k)} - \overline{K}^{\beta}_{m}\mathcal{D}_{\mu(k)}\right)^T$$

$$\overline{\mathcal{P}}_{m,\mu(k+1)} \triangleq \mathcal{N}_m P_{m,\mu(k+1)} N^T_m - sym\{N_m R^T_m\}$$

$$\phi^{\alpha}_{m,\mu(k)} \triangleq -\sigma \mathcal{P}_{m,\mu(k)} + \overline{F}^T_{\alpha}\overline{F}_{\alpha} - \Lambda_m J_1 + \zeta^{-1} X^T X$$

$$\Phi^{\alpha}_{1\,m,\mu(k)} \triangleq \begin{bmatrix} \phi^{\alpha}_{m,\mu(k)} & \Lambda_m J_2 \\ * & -\Lambda_m \end{bmatrix}, \ \Phi^{\alpha}_{3\,m} \triangleq \begin{bmatrix} \overline{B}^T_{\alpha} R^T_m \\ \overline{E}^T_{\alpha} R^T_m \end{bmatrix}$$

$$\mathcal{D}_{\mu(k)} \triangleq \overline{D}_{\mu(k)} - \begin{bmatrix} \triangle_{\mu(k)} \triangle(k)(I_N \otimes D) & 0 \end{bmatrix}$$

$$\mathcal{A}^{\alpha}_{m,\mu(k)} \triangleq \overline{A}^{\alpha}_{m,\mu(k)} - Z^T \overline{X}, \ X \triangleq \begin{bmatrix} \Gamma(I_N \otimes D) & 0 \end{bmatrix}$$

$$Y^{\beta}_m \triangleq R_m \mathcal{Z}^T - \overline{K}^{\beta}_m \triangle_{\mu(k)}, \ Z \triangleq \begin{bmatrix} 0 & \triangle_{\mu(k)} \end{bmatrix}$$

$$\overline{X} \triangleq [\triangle(\mathrm{k})(\mathrm{I_N} \otimes \mathrm{D}) \quad 0], \ R_m \triangleq \mathrm{diag}\{\mathrm{R_{1m}}, \mathrm{R_{2m}}\}$$

$$J_1 \triangleq \mathrm{diag}\left\{\upsilon^-_1 \upsilon^+_1, \ldots, \upsilon^-_{n_x N}\upsilon^+_{n_x N}\right\}$$

$$J_2 \triangleq \mathrm{diag}\left\{\frac{\upsilon^-_1 + \upsilon^+_1}{2}, \ldots, \frac{\upsilon^-_{n_x N} + \upsilon^+_{n_x N}}{2}\right\}$$

$$R_{1m} \triangleq \mathrm{diag}\{\mathrm{R_{1m,1}}, \ldots, \mathrm{R_{1m,N}}\}$$

$$R_{2m} \triangleq \mathrm{diag}\{\mathrm{R_{2m,1}}, \ldots, \mathrm{R_{2m,N}}\}$$

$$\overline{K}^{\beta}_{1m} \triangleq \mathrm{diag}\left\{\overline{\mathrm{K}}^{\beta}_{\mathrm{1m,1}}, \ldots, \overline{\mathrm{K}}^{\beta}_{\mathrm{1m,N}}\right\}$$

$$\overline{K}^{\beta}_{2m} \triangleq \mathrm{diag}\left\{\overline{\mathrm{K}}^{\beta}_{\mathrm{2m,1}}, \ldots, \overline{\mathrm{K}}^{\beta}_{\mathrm{2m,N}}\right\}$$

then, one can conclude that the EES (11) is GUES with an $\mathcal{H}_\infty$ performance level $\overline{\gamma}$. Furthermore, the specific form of the state estimators gains are displayed as

$$K^{\beta}_{1\,m} \triangleq R^{-1}_{1m}\overline{K}^{\beta}_{1\,m}, \ K^{\beta}_{2\,m} \triangleq R^{-1}_{2m}\overline{K}^{\beta}_{2\,m}.$$

*Proof:* It can be inferred that $\triangle^T(k)\triangle(k) \leq \Gamma^T\Gamma$ from $|\upsilon_n(k)| \leq \overline{\kappa}_n$ for $\forall n \in \{1, 2, \ldots, N\}$. Moreover, based on the fact that

$$\left(\mathcal{N}_m P_{m,\mu(k+1)} - R_m\right)\mathcal{P}^{-1}_{m,\mu(k+1)} \times \left(N_m P_{m,\mu(k+1)} - R_m\right)^T \geq 0,$$

one can deduce directly

$$-\mathcal{R}_m \mathcal{P}^{-1}_{m,\mu(k+1)} \mathcal{R}^{\mathcal{T}}_m \leq \mathcal{N}_m \mathcal{P}_{m,\mu(k+1)} N^T_m - sym\{N_m R^T_m\}.$$

In view of the candidate Lyapunov function (12) for the EES (11), we have

$$\begin{aligned} &V_m(e(k+1), \mu(k+1)) - \sigma V_m(e(k), \mu(k)) + \Xi_k \\ &= \left(\mathbb{A}^{\alpha\beta}_{m,\mu(k)} e(k) + \mathbb{B}^{\alpha}\overline{f}(e(k)) + \mathbb{E}^{\alpha}\omega(k)\right)^T \mathcal{P}_{m,\mu(k+1)} \\ &\quad \times \left(\mathbb{A}^{\alpha\beta}_{m,\mu(k)} e(k) + \mathbb{B}^{\alpha}\overline{f}(e(k)) + \mathbb{E}^{\alpha}\omega(k)\right) \\ &\quad - \sigma e^T(k)\mathcal{P}_{m,\mu(k)} e(k) + (\mathbb{F}^{\alpha} e(k))^T(\mathbb{F}^{\alpha} e(k)) \\ &\quad - \gamma^2 \omega^T(k)\omega(k). \end{aligned} \tag{21}$$

For function $f(e(k))$, note that the following inequality can derived from the Assumption 2

$$\begin{bmatrix} e(k) \\ \overline{f}(e(k)) \end{bmatrix}^T \begin{bmatrix} -\Lambda_m J_1 & \Lambda_m J_2 \\ * & -\Lambda_m \end{bmatrix} \begin{bmatrix} e(k) \\ \overline{f}(e(k)) \end{bmatrix} \geq 0. \tag{22}$$

Defining $\phi(k) \triangleq \begin{bmatrix} e^T(k) & \overline{f}^T(e(k)) & \omega^T(k) \end{bmatrix}^T$, in light of (22), one can obtain that

$$\begin{aligned} &V_m(e(k+1), \mu(k+1)) - \sigma V_m(e(k), \mu(k)) + \Xi_k \\ &\leq \phi^T(k)\Psi^{\alpha\beta}_{m,\mu(k)}\phi(k) \end{aligned}$$

where

$$\Psi^{\alpha\beta}_{m,\mu(k)} \triangleq \begin{bmatrix} \psi^{\alpha\beta}_{11\,m,\mu(k)} & \psi^{\alpha\beta}_{12\,m,\mu(k)} & \psi^{\alpha\beta}_{13\,m,\mu(k)} \\ * & \psi^{\alpha}_{22\,m,\mu(k)} & \psi^{\alpha}_{23\,m,\mu(k)} \\ * & * & \psi^{\alpha}_{33\,m,\mu(k)} \end{bmatrix}$$

$$\begin{aligned} \psi^{\alpha\beta}_{11\,m,\mu(k)} &\triangleq \left(\mathbb{A}^{\alpha\beta}_{m,\mu(k)}\right)^T \mathcal{P}_{m,\mu(k+1)}\left(\mathbb{A}^{\alpha\beta}_{m,\mu(k)}\right) \\ &\quad - \sigma P_{m,\mu(k)} + \overline{F}^T_{\alpha}\overline{F}_{\alpha} - \Lambda_m J_1 \\ \psi^{\alpha}_{23\,m,\mu(k)} &\triangleq (\mathbb{B}^{\alpha})^T \mathcal{P}_{m,\mu(k+1)}\mathbb{E}^{\alpha} \\ \psi^{\alpha}_{33\,m,\mu(k)} &\triangleq (\mathbb{E}^{\alpha})^T \mathcal{P}_{m,\mu(k+1)}\mathbb{E}^{\alpha} - \gamma^2 I \\ \psi^{\alpha\beta}_{13\,m,\mu(k)} &\triangleq \left(\mathbb{A}^{\alpha\beta}_{m,\mu(k)}\right)^T \mathcal{P}_{m,\mu(k+1)}\mathbb{E}^{\alpha} \\ \psi^{\alpha}_{22\,m,\mu(k)} &\triangleq (\mathbb{B}^{\alpha})^T \mathcal{P}_{m,\mu(k+1)}\mathbb{B}^{\alpha} - \Lambda_m \\ \psi^{\alpha\beta}_{12\,m,\mu(k)} &\triangleq \left(\mathbb{A}^{\alpha\beta}_{m,\mu(k)}\right)^T \mathcal{P}_{m,\mu(k+1)}\mathbb{B}^{\alpha} + \Lambda_m J_2. \end{aligned}$$

In the follows, utilizing the Schur complement, and pre- and post-multiplying $\mathrm{diag}\{I, I, I, R_m\}$ and its transpose, subsequently, with the employment of Lemma 2, one can attain that $\Psi^{\alpha\beta}_{m,\mu(k)} < 0$ is satisfied with the establishment of conditions (19) and (20). Additionally, it can be observed obviously that condition (18) is equivalent to (14). It finishes the proof. ■

## IV. An Illustrative Example

In this section, the reliability and validity of the proposed estimator are confirmed by the given simulation example. Several possible factors may affect the $\mathcal{H}_\infty$ performance level, such as the quantization density and the change rates $\rho$ as well as $\sigma$, and the assessment and analysis of the impact we focus on are supported by the results obtained.

Consider the investigated fuzzy CNNs (1) with four nodes, and each one contains two neurons. The switching connection topologies $G_1$ and $G_2$ are exhibited in Fig. 3,

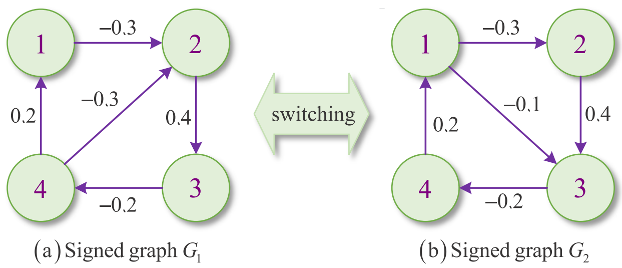


Fig. 3. The switching topologies $G_1$ and $G_2$.

in which the node set includes two subsets, i.e., $\mathcal{M}_1=\{1,4\}$ and $\mathcal{M}_2=\{2,3\}$. Evidently, the discussed weighted signed graphs are structurally balanced according to Definition 1, and their respective Laplacian matrices can be written as

$$\mathcal{L}_1=\begin{bmatrix}0.2 & 0 & 0 & -0.2\\ 0.3 & 0.6 & 0 & 0.3\\ 0 & -0.4 & 0.4 & 0\\ 0 & 0 & 0.2 & 0.2\end{bmatrix}$$
$$\mathcal{L}_2=\begin{bmatrix}0.2 & 0 & 0 & -0.2\\ 0.3 & 0.3 & 0 & 0\\ 0.1 & -0.4 & 0.5 & 0\\ 0 & 0 & 0.2 & 0.2\end{bmatrix}.$$

Afterwards, $\Phi=\mathrm{diag}\{-1,1,1,-1\}$ is selected, and the connection topology switching is accomplished by means of a time-varying signal $\delta(k)$, whose parameters are chosen as $T_p=8$, $\tau_p=6$, $\rho=1.001$, $\sigma=0.999$. For each node given by (1), its system parameters are in the form of

$$A_1=\mathrm{diag}\{0.45,0.675\}, A_2=\mathrm{diag}\{0.35,0.455\}$$
$$c=1, B_1=\begin{bmatrix}0.6 & 0.036\\ 0.084 & -0.36\end{bmatrix}, B_2=\begin{bmatrix}0.45 & 0.03\\ 0.06 & -0.3\end{bmatrix}$$
$$D=\begin{bmatrix}0.3 & 0.3\end{bmatrix}, E_{i,1}=\begin{bmatrix}0.2\\ 0.4\end{bmatrix}, E_{i,2}=\begin{bmatrix}0.22\\ 0.44\end{bmatrix}$$
$$F_1=\begin{bmatrix}0.02 & 0.03\end{bmatrix}, F_2=\begin{bmatrix}0.03 & 0.02\end{bmatrix}, i=1,2,3,4.$$

The $\mathcal{H}_\infty$ disturbance attenuation index $\gamma=0.78$ and the external disturbance input $\omega(k)=0.1\exp(-0.04k)\sin(0.4k)$ are made use of to explain the performance level. According to Assumption 2, $f(x(k))=\tanh(x(k))$ satisfying (4) with $\nu_i^-=0$ and $\nu_i^+=1$ is given as the odd activation function. Besides, the data of each node is assumed to be quantified with the common standard, and it follows that the overall quantizer density can be got as $\eta=\mathrm{diag}\{0.9, 0.9, 0.9, 0.9\}$. Then, in the light of the approach presented in Theorem 2, the desired estimator gain under the RRP can be computed as

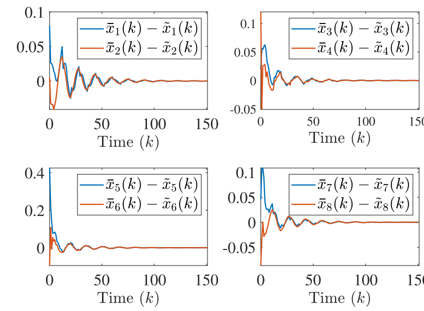


Fig. 4. The estimation error trajectories of all neurons.

$$K_{11}^1=\mathrm{diag}\left\{K_{11}^{1(1)},K_{11}^{1(2)},K_{11}^{1(3)},K_{11}^{1(4)}\right\}$$
$$K_{11}^2=\mathrm{diag}\left\{K_{11}^{2(1)},K_{11}^{2(2)},K_{11}^{2(3)},K_{11}^{2(4)}\right\}$$
$$K_{12}^1=\mathrm{diag}\left\{K_{12}^{1(1)},K_{12}^{1(2)},K_{12}^{1(3)},K_{12}^{1(4)}\right\}$$
$$K_{12}^2=\mathrm{diag}\left\{K_{12}^{2(1)},K_{12}^{2(2)},K_{12}^{2(3)},K_{12}^{2(4)}\right\}$$
$$K_{11}^{1(1)}=\begin{bmatrix}1.7418\\ 0.2414\end{bmatrix}, K_{11}^{1(2)}=\begin{bmatrix}0.7012\\ -0.0051\end{bmatrix}$$
$$K_{11}^{1(3)}=\begin{bmatrix}1.4622\\ -0.0706\end{bmatrix}, K_{11}^{1(4)}=\begin{bmatrix}1.4174\\ 0.2448\end{bmatrix}$$
$$K_{11}^{2(1)}=\begin{bmatrix}0.7972\\ 0.1268\end{bmatrix}, K_{11}^{2(2)}=\begin{bmatrix}-0.1481\\ -0.1546\end{bmatrix}$$
$$K_{11}^{2(3)}=\begin{bmatrix}0.3247\\ 0.0847\end{bmatrix}, K_{11}^{2(4)}=\begin{bmatrix}0.7577\\ 0.0623\end{bmatrix}$$
$$K_{12}^{1(1)}=\begin{bmatrix}1.6132\\ 0.1961\end{bmatrix}, K_{12}^{1(2)}=\begin{bmatrix}1.0463\\ -0.1873\end{bmatrix}$$
$$K_{12}^{1(3)}=\begin{bmatrix}0.9776\\ 0.0161\end{bmatrix}, K_{12}^{1(4)}=\begin{bmatrix}1.6468\\ 0.2863\end{bmatrix}$$
$$K_{12}^{2(1)}=\begin{bmatrix}0.7896\\ 0.0951\end{bmatrix}, K_{12}^{2(2)}=\begin{bmatrix}0.6638\\ 0.1878\end{bmatrix}$$
$$K_{12}^{2(3)}=\begin{bmatrix}1.1775\\ -0.0533\end{bmatrix}, K_{12}^{2(4)}=\begin{bmatrix}0.6676\\ 0.1365\end{bmatrix}$$
$$K_{21}^1=\mathrm{diag}\{0.9577,0.9976,0.9857,0.9914\}$$
$$K_{21}^2=\mathrm{diag}\{1.0072,0.9996,0.9991,1.0014\}$$
$$K_{22}^1=\mathrm{diag}\{0.9873,0.991,0.9927,0.9859\}$$
$$K_{22}^2=\mathrm{diag}\{0.9995,1.0006,0.9978,0.9994\}.$$

The initial value of the augment system (8) and its estimator are given as $\widehat{x}(0)=0_{12}$, $\widetilde{x}(0)=[0.2;-0.2;0.2;-0.5;\ 0.8;-0.4;-0.3;0;0;0;0]$. In this way, under the possible mode evolution governed by the PDT switching signal $\delta(k)$, the resulting estimation error trajectories of all neurons and the output responses $\widetilde{z}_i(k)$ belonging to the node $i$ are depicted in Figs. 4 and 5 with the normalized membership functions

$$\xi_1(\overline{x}_1(k))=\begin{cases}0.5\left(1+\frac{\overline{x}_1(k)}{2}\right), & |\overline{x}_1(k)|\le 2\\ 0, & \text{otherwise}\end{cases}$$
$$\xi_2(\overline{x}_1(k))=1-\xi_1(\overline{x}_1(k)).$$

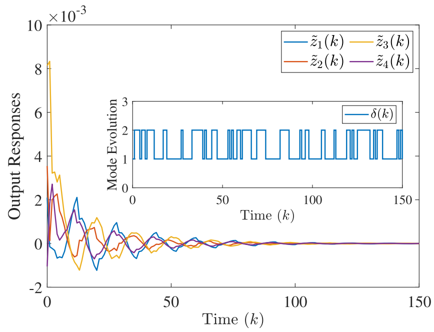


Fig. 5. State trajectories of $\widetilde{z}_i(k), i = 1, 2, 3, 4$ subject to the signal $\delta(k)$.

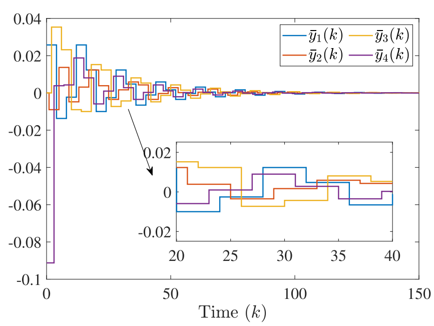


Fig. 6. Measurement output transmitted to the estimator after processing by RRP.

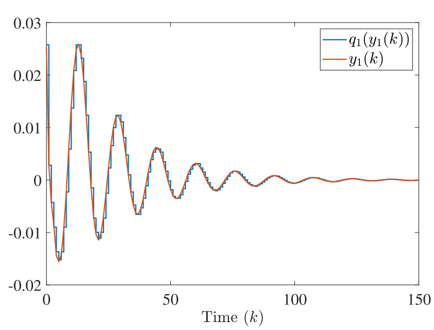


Fig. 7. Measurement output $y_1(k)$ and its quantized value $q_1(y_1(k))$.

As is observed apparently from the above results, all the response curves gradually converge to zero, namely the designed estimator has the ability to follow the node states rapidly, and the stability of EES can be realized at an exponential convergence rate in global-uniform sense, which verifies that the theoretical results are indeed correct and the intended stability goal is reached. Besides, for the sake of highlighting the effects of transmission protocol, measurement output values transmitted to the estimator of different nodes are figured in Fig. 6, wherein, Node 1 is permitted to fetch new data when $k = 20$, and then its data is locked to maintain at the same level during a traversal period $\mathbb{T} = 4$. Next, similar procedures for Nodes 2, 3, and 4 are carried out in sequence, and it should be noticed that only one node can execute the update program at the moment $k$. As far as Node 1 is concerned, as shown in Fig. 7, the quantized values $q_1(y_1(k))$ are stepped in contrast with the unprocessed amplitude of original $y_1(k)$, which

TABLE I
THE OPTIMAL $\mathcal{H}_\infty$ PERFORMANCE LEVEL $\overline{\gamma}_{\min}$ WITH DIFFERENT $\rho$, $\sigma$ AND $\eta_n$

| $\overline{\gamma}_{\min}$ | | $\sigma = 0.991$ | $\sigma = 0.993$ | $\sigma = 0.996$ |
|---|---|---|---|---|
| $\eta_n = 0.85$ | $\rho = 1.003$ | 0.7113 | 0.7326 | 0.799 |
| | $\rho = 1.004$ | 0.7503 | 0.7805 | 0.947 |
| | $\rho = 1.005$ | 0.7822 | 0.8421 | 1.2012 |
| $\eta_n = 0.95$ | $\rho = 1.003$ | 0.3095 | 0.3097 | 0.3472 |
| | $\rho = 1.004$ | 0.3259 | 0.3311 | 0.4185 |
| | $\rho = 1.005$ | 0.3436 | 0.3586 | 0.5577 |

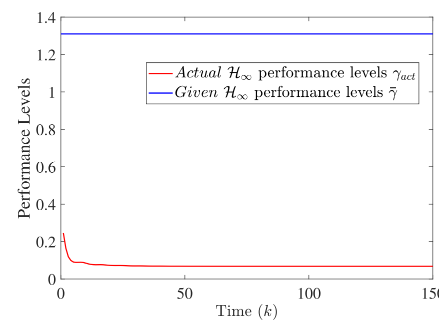


Fig. 8. Actual $\mathcal{H}_\infty$ performance level $\gamma_{act}$ and the prescribed one $\overline{\gamma}$ over time.

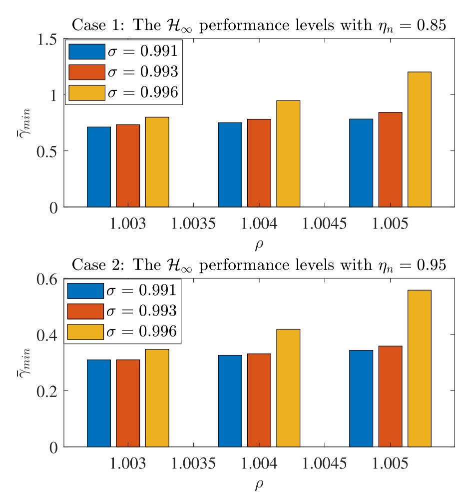


Fig. 9. The variation trend of $\overline{\gamma}_{\min}$ with different $\rho$, $\sigma$ and $\eta_n$..

means that the quantizer does play a part in processing the samples. As a consequence, it is feasible to reduce the burden of channels significantly with the quantified information transmission arranged by RRP.

In what follows, these statistics in Table I depict the influence of the different decay rates $\rho$, $\sigma$ and the quantization density $\eta_n$ on the $\mathcal{H}_\infty$ performance level of the investigated EES, which leads us to the conclusion that a higher level $\overline{\gamma}_{\min}$, namely a worse anti-disturbed ability the systems own, can be obtained with the increase in $\rho$ or $\sigma$ under a fixed value of $\eta_n$, and the overall performance level $\overline{\gamma}_{\min}$ is lower than before with the increase in $\eta_n$, which means that the robust $\mathcal{H}_\infty$ performance of EES can be improved by adjusting the density $\eta_n$ in a certain range. Moreover, to draw such a relationship among $\rho$, $\sigma$, $\eta_n$ more vividly, Fig. 9 is given based on these statistics, which are calculated under the premise that the derived matrix inequality conditions in Theorem 2 hold. Obviously, there is an increment of $\overline{\gamma}_{\min}$ as $\rho$ and $\sigma$ decrease or $\eta_n$ increase to a certain level. Furthermore, the $\mathcal{H}_\infty$ disturbance attenuation level of the actual system under the zero-initial conditions is given out in Fig. 8, and the concrete index in the simulation length of time is examined as

$$\sqrt{\frac{\sum_{k=0}^{150} \widetilde{z}^T(k)\widetilde{z}(k)}{\sum_{k=0}^{150} \omega^T(k)\omega(k)}} = 0.068 \, < \, \overline{\gamma} = 1.3101.$$

Clearly, the $\mathcal{H}_\infty$ performance level $\gamma_{act}$ for the actual system is less than the given value $\overline{\gamma}$ in the whole time, which confirms that the requirement in Definition 4 is satisfied.

## V. Conclusion

In this paper, the $\mathcal{H}_\infty$ state estimation issues for a class of discrete-time nonlinear CNNs with the switching NT and opposite interactions have been addressed. The PDT-switched weighted signed graph has been introduced to depict the potential evolution of cooperation-competition-based connection topology among nodes. A classic T-S fuzzy model has been applied to handle the nonlinear factors of the investigated system. Moreover, a feasible scheme has been presented to protect the communication from network-deduced problems effectively, by which measured data is assigned to a logarithmic quantizer and then sent to the estimator by obeying RRP. Additionally, sufficient criteria have been provided to guarantee the exponential stability of EES in the global-uniform sense with an expected $\mathcal{H}_\infty$ performance level. Finally, the validity and superiority of the proposed method have been illustrated by a verification example. Furthermore, future work will extend the proposed strategy to complex coupled networks with singular perturbation in the finite-time sense.

## References


[1] X. Wang et al., "Novel heterogeneous mode-dependent impulsive synchronization for piecewise TS fuzzy probabilistic coupled delayed neural networks," *IEEE Trans. Fuzzy Syst.*, vol. 30, no. 7, pp. 2142–2156, Jul. 2022.

[2] J.-L. Wang, M. Xu, H.-N. Wu, and T. Huang, "Finite-time passivity of coupled neural networks with multiple weights," *IEEE Trans. Netw. Sci. Eng.*, vol. 5, no. 3, pp. 184–197, Jul.–Sep. 2018.

[3] L.-h. Zhao, S. Wen, M. Xu, K. Shi, S. Zhu, and T. Huang, "PID control for output synchronization of multiple output coupled complex networks," *IEEE Trans. Netw. Sci. Eng.*, vol. 9, no. 3, pp. 1553–1566, May/Jun. 2022.

[4] H. Rao, F. Liu, H. Peng, Y. Xu, and R. Lu, "Observer-based impulsive synchronization for neural networks with uncertain exchanging information," *IEEE Trans. Neural Netw. Learn. Syst.*, vol. 31, no. 10, pp. 3777–3787, Oct. 2020.

[5] Y. Lou, L. Wang, and G. Chen, "Toward stronger robustness of network controllability: A snapback network model," *IEEE Trans. Circuits Syst. I., Regular Papers*, vol. 65, no. 9, pp. 2983–2991, Sep. 2018.

[6] H. Shen, X. Hu, J. Wang, J. Cao, and W. Qian, "Non-fragile $\mathcal{H}_\infty$ synchronization for Markov jump singularly perturbed coupled neural networks subject to double-layer switching regulation," *IEEE Trans. Neural Netw. Learn. Syst.*, to be published, doi: 10.1109/TNNLS.2021.3107607.

[7] H. K. Kwan and Y. Cai, "A fuzzy neural network and its application to pattern recognition," *IEEE Trans. Fuzzy Syst.*, vol. 2, no. 3, pp. 185–193, Aug. 1994.

[8] H. Zhang, J. Wang, Z. Wang, and H. Liang, "Mode-dependent stochastic synchronization for Markovian coupled neural networks with time-varying mode-delays," *IEEE Trans. Neural Netw. Learn. Syst.*, vol. 26, no. 11, pp. 2621–2634, Nov. 2015.

[9] Y. Luo, Z. Wang, Y. Chen, and X. Yi, "$\mathcal{H}_\infty$ state estimation for coupled stochastic complex networks with periodical communication protocol and intermittent nonlinearity switching," *IEEE Trans. Netw. Sci. Eng.*, vol. 8, no. 2, pp. 1414–1425, Apr.–Jun. 2021.

[10] R. Tang, X. Yang, and X. Wan, "Finite-time cluster synchronization for a class of fuzzy cellular neural networks via non-chattering quantized controllers," *Neural Netw.*, vol. 113, pp. 79–90, May 2019.

[11] C. Chen, L. Li, H. Peng, and Y. Yang, "Fixed-time synchronization of memristor-based BAM neural networks with time-varying discrete delay," *Neural Netw.*, vol. 96, pp. 47–54, Dec. 2017.

[12] B. Liu and T. Chen, "Consensus in networks of multiagents with cooperation and competition via stochastically switching topologies," *IEEE Trans. Neural Netw. Learn. Syst.*, vol. 19, no. 11, pp. 1967–1973, Nov. 2008.

[13] H.-X. Hu, Q. Xuan, W. Yu, C.-G. Zhang, and G. Xie, "Second-order consensus for heterogeneous multi-agent systems in the cooperation–competition network: A hybrid adaptive and pinning control approach," *Nonlinear Anal. Hybrid. Syst.*, vol. 20, pp. 21–36, May 2016.

[14] H.-X. Hu, G. Wen, W. Yu, J. Cao, and T. Huang, "Finite-time coordination behavior of multiple Euler–Lagrange systems in cooperation-competition networks," *IEEE Trans. Cybern.*, vol. 49, no. 8, pp. 2967–2979, Aug. 2019.

[15] G. Wen, X. Yu, W. Yu, and J. Lu, "Coordination and control of complex network systems with switching topologies: A survey," *IEEE Trans. Syst. Man, Cybern. Syst.*, vol. 51, no. 10, pp. 6342–6357, Oct. 2021.

[16] H. Wang, X. Chen, and J. Wang, "$\mathcal{H}_\infty$ sliding mode control for PDT-switched nonlinear systems under the dynamic event-triggered mechanism," *Appl. Math. Comput.*, vol. 412, Jan. 2022, Art. no. 126474.

[17] S. Shi, Z. Fei, T. Wang, and Y. Xu, "Filtering for switched T–S fuzzy systems with persistent dwell time," *IEEE Trans. Cybern.*, vol. 49, no. 5, pp. 1923–1931, May 2019.

[18] H. Shen, M. Xing, Z. Wu, J. Cao, and T. Huang, "$l_2 - l_\infty$ state estimation for persistent dwell-time switched coupled networks subject to round-robin protocol," *IEEE Trans. Neural Netw. Learn. Syst.*, vol. 32, no. 5, pp. 2002–2014, May 2021.

[19] J. Wang, Z. Huang, Z. Wu, J. Cao, and H. Shen, "Extended dissipative control for singularly perturbed PDT switched systems and its application," *IEEE Trans. Circuits Syst. I., Regular Papers*, vol. 67, no. 12, pp. 5281–5289, Dec. 2020.

[20] H. Shen, M. Xing, Z.-G. Wu, S. Xu, and J. Cao, "Multiobjective fault-tolerant control for fuzzy switched systems with persistent dwell time and its application in electric circuits," *IEEE Trans. Fuzzy Syst.*, vol. 28, no. 10, pp. 2335–2347, Oct. 2020.

[21] J. A. Meda-Campaña, J. Rodríguez-Valdez, T. Hernández-Cortés, R. Tapia-Herrera, and V. Nosov, "Analysis of the fuzzy controllability property and stabilization for a class of T–S fuzzy models," *IEEE Trans. Fuzzy Syst.*, vol. 23, no. 2, pp. 291–301, Apr. 2015.

[22] J. Wang, C. Yang, J. Xia, Z.-G. Wu, and H. Shen, "Observer-based sliding mode control for networked fuzzy singularly perturbed systems under weighted try-once-discard protocol," *IEEE Trans. Fuzzy Syst.*, vol. 30, no. 6, pp. 1889–1899, Jun. 2022.

[23] D. Chen, X. Liu, and W. Yu, "Finite-time fuzzy adaptive consensus for heterogeneous nonlinear multi-agent systems," *IEEE Trans. Netw. Sci. Eng.*, vol. 7, no. 4, pp. 3057–3066, Oct.–Dec. 2020.

[24] Y. Zhang, L. Ma, G. Wang, C. Yang, L. Zhou, and W. Dai, "Observer-based control for the two-time-scale cyber-physical systems: The dual-scale DoS attacks case," *IEEE Trans. Netw. Sci. Eng.*, vol. 8, no. 4, pp. 3369–3379, Oct.–Dec. 2021.

[25] L. Zou, Z. Wang, H. Gao, and X. Liu, "State estimation for discrete-time dynamical networks with time-varying delays and stochastic disturbances under the round-robin protocol," *IEEE Trans. Neural Netw. Learn. Syst.*, vol. 28, no. 5, pp. 1139–1151, May 2017.

[26] L. Wang and X. Wang, "New conditions for synchronization in dynamical communication networks," *Syst. Control Lett.*, vol. 60, no. 4, pp. 219–225, Apr. 2011.

[27] X. Jin, W. Du, W. He, L. Kocarev, Y. Tang, and J. Kurths, "Twisting-based finite-time consensus for Euler–Lagrange systems with an event-triggered strategy," *IEEE Trans. Netw. Sci. Eng.*, vol. 7, no. 3, pp. 1007–1018, Jul.–Sep. 2020.

[28] S. Wang, Y. Cao, S. Wen, Z. Guo, T. Huang, and Y. Chen, "Projective synchroniztion of neural networks via continuous/periodic event-based sampling algorithms," *IEEE Trans. Netw. Sci. Eng.*, vol. 7, no. 4, pp. 2746–2754, Oct.–Dec. 2020.

[29] Y. Dong, Y. Song, and G. Wei, "Efficient model-predictive control for nonlinear systems in interval type-2 T-S fuzzy form under round-robin protocol," *IEEE Trans. Fuzzy Syst.*, vol. 30, no. 1, pp. 63–74, Jan. 2022.

[30] X. Wan, Y. Li, Y. Li, and M. Wu, "Finite-time $\mathcal{H}_\infty$ state estimation for two-time-scale complex networks under stochastic communication protocol," *IEEE Trans. Neural Netw. Learn. Syst.*, vol. 33, no. 1, pp. 25–36, Jan. 2022.

[31] X. Wan, Z. Wang, M. Wu, and X. Liu, "$\mathcal{H}_\infty$ state estimation for discrete-time nonlinear singularly perturbed complex networks under the round-robin protocol," *IEEE Trans. Neural Netw. Learn. Syst.*, vol. 30, no. 2, pp. 415–426, Feb. 2019.

[32] S. Liu, Z. Wang, G. Wei, and M. Li, "Distributed set-membership filtering for multirate systems under the round-robin scheduling over sensor networks," *IEEE Trans. Cybern.*, vol. 50, no. 5, pp. 1910–1920, May 2020.

[33] Z. Wang, Y. Xu, R. Lu, and H. Peng, "Finite-time state estimation for coupled Markovian neural networks with sensor nonlinearities," *IEEE Trans. Neural Netw. Learn. Syst.*, vol. 28, no. 3, pp. 630–638, Mar. 2017.

[34] W. Li, Y. Jia, and J. Du, "Variance-constrained state estimation for nonlinearly coupled complex networks," *IEEE Trans. Cybern.*, vol. 48, no. 2, pp. 818–824, Feb. 2018.

[35] F. Harary, "On the notion of balance of a signed graph," *Michigan Math. J.*, vol. 2, no. 2, pp. 143–146, 1953.

[36] Z. Meng, G. Shi, K. H. Johansson, M. Cao, and Y. Hong, "Behaviors of networks with antagonistic interactions and switching topologies," *Automatica*, vol. 73, pp. 110–116, Nov. 2016.

[37] J. Liu, H. Li, J. Ji, and J. Luo, "Group-bipartite consensus in the networks with cooperative-competitive interactions," *IEEE Trans. Circuits Syst. II, Exp. Briefs*, vol. 67, no. 12, pp. 3292–3296, Dec. 2020.

[38] M. Wang, H.-K. Lam, J. Qiu, H. Yan, and Z. Li, "Fuzzy-affine-model-based filtering design for continuous-time roesser-type 2-D nonlinear systems," *IEEE Trans. Cybern.*, to be published, doi: 10.1109/TCYB.2022.3163191.


**Hao Shen** (Member, IEEE) received the Ph.D. degree in control theory and control engineering from the Nanjing University of Science and Technology, Nanjing, China, in 2011. Since 2011, he has been with the Anhui University of Technology, Anhui, China, where he is currently a Professor. His research interests include stochastic hybrid systems, complex networks, fuzzy systems and control, and nonlinear control. He was on the Technical Program Committee of several international conferences. He is an Associate Editor for several international journals, including *Journal of The Franklin Institute*, *Applied Mathematics and Computation* and *Neural Processing Letters*. Prof. Shen was the recipient of the Highly Cited Researcher Award by Clarivate Analytics (formerly, Thomson Reuters) in 2019–2022.

**Yinsheng Song** is currently working toward the M.S. degree with the School of Electrical and Information Engineering, Anhui University of Technology, Anhui, China. His research interests include switched systems, fuzzy systems, and neural networks.

**Jing Wang** received the Ph.D. degree in power system and automation from Hohai University, Nanjing, China, in 2019. She is currently an Associate Professor with the School of Electrical and Information Engineering, Anhui University of Technology, China. Her research interests include Markov jump nonlinear systems, singularly perturbed systems, power systems, and nonlinear control.

**Ju H. Park** (Senior Member, IEEE) received the Ph.D. degree in electronics and electrical engineering from the Pohang University of Science and Technology (POSTECH), Pohang, Republic of Korea, in 1997. From May 1997 to February 2000, he was a Research Associate with Engineering Research Center-Automation Research Center, POSTECH. In March 2000, he joined Yeungnam University, Kyongsan, Republic of Korea, where he is currently the Chuma Chair Professor. He has authored or coauthored a number of articles in his research interests which include robust control and filtering, neural/complex networks, fuzzy systems, multiagent systems, and chaotic systems. He is a coauthor of the monographs *Recent Advances in Control and Filtering of Dynamic Systems with Constrained Signals* (New York, NY, USA: Springer-Nature, 2018) and *Dynamic Systems With Time Delays: Stability and Control* (New York, NY, USA: Springer-Nature, 2019) and is also the Editor of an edited volume *Recent Advances in Control Problems of Dynamical Systems and Networks* (New York: Springer-Nature, 2020). In 2015, he was the recipient of the Highly Cited Researchers Award by Clarivate Analytics (formerly, Thomson Reuters) and was listed in three fields, Engineering, Computer Sciences, and Mathematics from 2019 to 2022. He was also the Editor of the *International Journal of Control, Automation and Systems*. He is a Subject Editor/Advisory Editor/Associate Editor/Editorial Board Member of several international journals, including *IET Control Theory & Applications, Applied Mathematics and Computation, Journal of The Franklin Institute, Nonlinear Dynamics, Engineering Reports, Cogent Engineering*, IEEE TRANSACTION ON FUZZY SYSTEMS, IEEE TRANSACTION ON NEURAL NETWORKS AND LEARNING SYSTEMS, and IEEE TRANSACTION ON CYBERNETICS. Dr. Park is a Fellow of the Korean Academy of Science and Technology.